Efficient Dye-Sensitized Photovoltaic Wires Based on an Organic Redox Electrolyte

ARTICLE *in* JOURNAL OF THE AMERICAN CHEMICAL SOCIETY · JULY 2013

Impact Factor: 12.11 · DOI: 10.1021/ja405012w · Source: PubMed

6 AUTHORS, INCLUDING:

Zhibin Yang
University of Washington Seattle
58 PUBLICATIONS **1,547** CITATIONS
SEE PROFILE

Houpu Li
Fudan University
23 PUBLICATIONS **438** CITATIONS
SEE PROFILE

Longbin Qiu
Fudan University
52 PUBLICATIONS **1,239** CITATIONS
SEE PROFILE

Hao Sun
Fudan University
27 PUBLICATIONS **343** CITATIONS
SEE PROFILE

JACS
JOURNAL OF THE AMERICAN CHEMICAL SOCIETY

Communication

pubs.acs.org/JACS

Efficient Dye-Sensitized Photovoltaic Wires Based on an Organic Redox Electrolyte

Shaowu Pan,[†,‡] Zhibin Yang,[†] Houpu Li,[†] Longbin Qiu,[†] Hao Sun,[†] and Huisheng Peng[†,‡,*]

[†]State Key Laboratory of Molecular Engineering of Polymers, Department of Macromolecular Science, and Laboratory of Advanced Materials, Fudan University, Shanghai 200438, China

[‡]School of Materials Science and Engineering, Tongji University, 4800 Caoan Road, Shanghai 201804, China

Supporting Information

ABSTRACT: An organic thiolate/disulfide redox couple with low absorption in the visible region was developed for use in fabricating novel dye-sensitized photovoltaic wires with an aligned carbon nanotube (CNT) fiber as the counter electrode. These flexible wire devices achieved a maximal energy conversion efficiency of 7.33%, much higher than the value of 5.97% for the conventional I^-/I_3^- redox couple. In addition, the aligned CNT fiber also greatly outperforms the conventional Pt counter electrode with a maximal efficiency of 2.06% based on the thiolate/disulfide redox couple.

Dye-sensitized solar cells (DSCs) have been widely studied as a promising new type of photovoltaic devices because of their easy fabrication, low cost, and flexibility compared with the conventional, rigid silicon wafer-based technology.[1] To further improve their energy conversion efficiencies, much effort has been devoted to optimization of components[2−6]and creative novel structures of DSCs.[7−9] The electrolyte that functions to transfer electrons from the counter electrode to the oxidized dye is a key component in the DSC, and the I^-/I_3^- redox couple has been generally used. Although this conventional redox couple works efficiently, disadvantages such as corrosion of the current collector (typically based on Ag or Cu) and partial absorption in the visible region has largely limited the applicable production of DSCs. Therefore, a lot of attention has been paid to discovering alternative redox couples for the future development of DSCs.[10−13] Among them, organic redox couples show promising advantages such as high efficiency and safety.

However, as another key component, the counter electrode (typically composed of Pt) exhibits very low catalytic activity toward organic redox couples such as the thiolate/disulfide redox couple.[14,15] The low fill factor is produced from a large reduction resistance of the disulfide on the standard platinized counter electrode, leading to a low energy conversion efficiency. This phenomenon indicates that Pt may be not suitable as a counter electrode to catalyze the organic redox couple. Therefore, highly catalytic counter electrode materials are urgently required. Some attempts have been made to explore carbon materials[16−19] and organic polymers as counter electrodes.[20,21] The DSCs appeared in a rigid, planar format, although organic redox couples were proposed to be particularly promising for making flexible DSCs.

In this work, a new organic redox couple showing negligible absorption in the visible region was developed for use in the fabrication of flexible dye-sensitized photovoltaic wires. An aligned carbon nanotube (CNT) fiber with high flexibility, tensile strength, and electrical conductivity serves as a counter electrode, and a Ti wire with perpendicularly aligned titania nanotubes functions as the working electrode. The two electrodes are intertwined together to form the wire cell (Figure 1). The design and use of an aligned CNT fiber as the counter

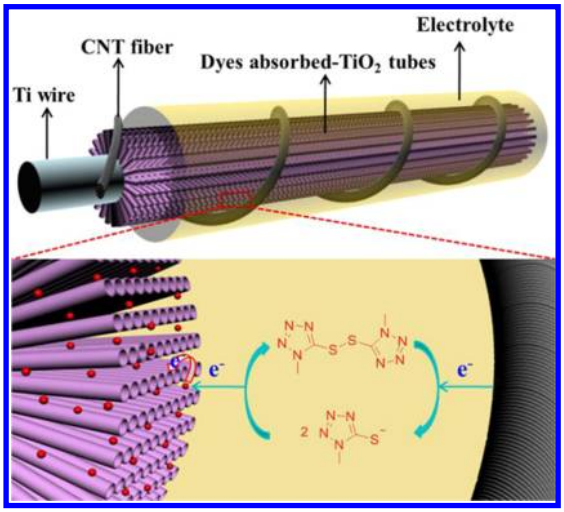

Figure 1. Schematic illustration of a photovoltaic wire with a CNT fiber as the counter electrode, a Ti wire impregnated with titania nanotubes as the working electrode, and the thiolate/disulfide redox couple as the electrolyte.

electrode effectively catalyzes the thiolate/disulfide redox couple with an energy conversion efficiency of 7.33%, which is much higher than the efficiency of 2.06% based on the Pt counter electrode under the same conditions. The use of the organic redox couple also proved to be critical in the development of the dye-sensitized photovoltaic wires. Corrosion due to the I^-/I_3^- redox couple decreases the energy conversion efficiency and lifetime in the photovoltaic wire more than in a conventional planar device, and also requires more complex fabrication. In addition, the novel dye-sensitized photovoltaic wire constructed from the organic redox couple shows much higher efficiency than the I^-/I_3^- redox couple under the same conditions with the

Received: May 18, 2013
Published: July 15, 2013

   dx.doi.org/10.1021/ja405012w | J. Am. Chem. Soc. 2013, 135, 10622−10625

aligned CNT fiber as the counter electrode. This photovoltaic wire is flexible, lightweight, and weaveable.

For this organic redox couple, the thiolate (T^-) and disulfide (T_2) components, whose structures are shown in Scheme 1, were

Scheme 1. Structures of the Thiolate (T^-) and Disulfide (T_2) Components of the Redox Couple

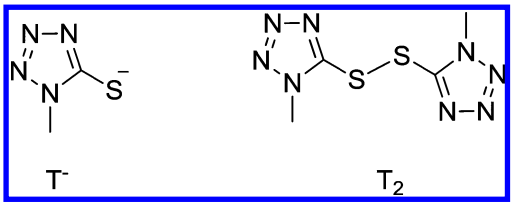

synthesized by neutralization of 5-mercapto-1-methyltetrazole with NMe_4OH and oxidation of 5-mercapto-1-methyltetrazole, respectively [for synthetic details, see the Experimental Section and Figures S1 and S2 in the Supporting Information (SI)]. The UV–vis spectra of the T^-/T_2 and I^-/I_3^- redox couples (Figure S3) show that the organic redox couple has less absorption in the visible region, which is widely known to be important for highly efficient DSCs.

To prepare the aligned CNT fiber, a CNT array was first synthesized by chemical vapor deposition, and continuous CNT sheets with a thickness of ~20 nm were then pulled out of the array.[22] Many layers of CNT sheets were stacked and further spun into a CNT fiber, typically using a microprobe rotation speed of 2000 rpm. The diameters of the CNT fibers were controlled from 25 to 100 μm by increasing the number of sheet layers from 2 to 25. Figure S4 shows a micrograph of the spinning process used to produce an aligned CNT fiber. Figure 2a shows a

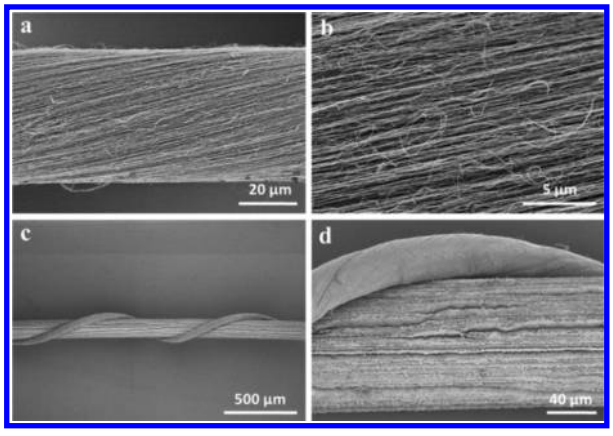

Figure 2. SEM images of (a, b) the CNT fiber and (c, d) part of the twisted photovoltaic wire at (a, c) low and (b, d) high magnification.

scanning electron microscopy (SEM) image of an aligned CNT fiber with a uniform diameter of 60 μm. A higher-magnification image (Figure 2b) further indicates that the CNTs are highly aligned along the twisting direction in the fiber. The resulting CNT fibers are lightweight, flexible, strong (tensile strength of 10^2–10^3 MPa), and conductive (electrical conductivity of 10^2–10^3 S cm^{-1}). They represent a new family of electrode materials for various optoelectronic and electronic microdevices.[23−25] Here their use as counter electrodes in DSCs was investigated.

A Ti wire with titania nanotubes perpendicularly aligned on the surface was used as the working electrode to fabricate the dye-sensitized photovoltaic wire. The titania nanotubes were grown by electrochemical anodization and had a length of 30 μm and diameters of 70–100 nm (Figure S5).[26] The modified Ti wire was immersed into a solution of N719 dye, and an aligned CNT fiber was twisted around the dye-absorbed working electrode. The photovoltaic wire could be sealed in a glass capillary tube or a flexible fluorinated ethylenepropylene tube with subsequent infiltration of the electrolyte by capillary force. Figure 2c shows a typical SEM image of a photovoltaic wire with pitch distance of 1 mm. The two fiber electrodes are in close contact with each other (Figure 2d), and the twist structure was well-maintained during bending, indicating the high stability and flexibility of the wire cell (Figure S6).

Figure 3 compares current density–voltage (J–V) curves of dye-sensitized photovoltaic wires having aligned CNT fibers with

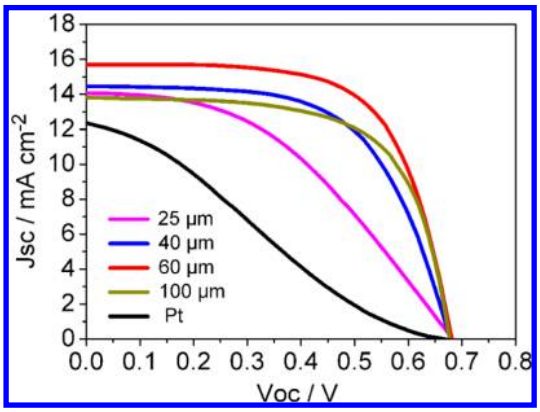

Figure 3. J–V curves of photovoltaic wires using CNT fibers with diameters of 25, 40, 60, and 100 μm or a Pt wire with diameter of 25 μm as counter electrodes, measured under AM 1.5 illumination using the same T^-/T_2 redox couple.

increasing diameters as counter electrodes and the T^-/T_2 redox couple as the electrolyte measured under AM 1.5 illumination. In this work, the surface of the top half of the photovoltaic wire was appropriately irradiated. The photovoltaic parameters [open-circuit voltage (V_{oc}), short-circuit current density (J_{sc}), fill factor (FF), and energy conversion efficiency (η)] are summarized at Table 1. The V_{oc} values were almost the same for the CNT fibers

Table 1. Photovoltaic Parameters in Figure 3

counter electrode	V_{oc} (mV)	J_{sc} (mA cm^{-2})	FF	η (%)
25 μm fiber	682	14.05	0.43	4.13
40 μm fiber	678	14.46	0.61	5.95
60 μm fiber	680	15.69	0.66	7.01
100 μm fiber	676	13.80	0.65	6.10
Pt wire	669	12.29	0.25	2.06

with different diameters. However, as the diameter increased from 25 to 60 μm, the average J_{sc} and FF values continuously increased from 14.05 to 15.69 mA/cm^2 and 0.43 to 0.66, respectively. As a result, η improved from 4.13% to 7.01%. With a further increase in the diameter to 100 μm, η decreased to 6.10%. The optimal diameter for the CNT fiber was 60 μm as a result of two opposite factors.[27] On one hand, larger CNT fibers have more catalytic sites. On the other hand, larger CNT fibers become less flexible, and the twisted structures are less uniform. In addition, a larger fiber shades more dyes from illumination. As a comparison, a Pt wire with a diameter of 25 μm was used as the counter electrode under the same conditions. The V_{oc} was similar

dx.doi.org/10.1021/ja405012w | J. Am. Chem. Soc. 2013, 135, 10622–10625

to those of the CNT fibers, but both J_{sc} and FF sharply decreased, producing a lower η of 2.06%. Notably, the photovoltaic parameters varied by less than 3% (e.g., η = 7.18 ± 0.17% at a CNT fiber diameter of 60 μm).

The catalytic activities of aligned CNT fibers and Pt wire with the T^-/T_2 redox couple were further studied by cyclic voltammetry (Figure 4). A pair of redox peaks should be

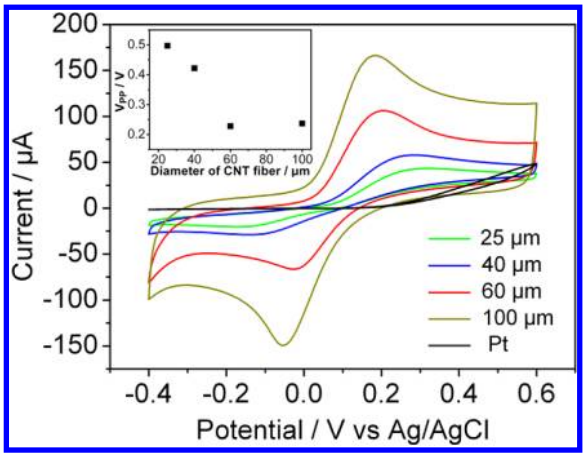

Figure 4. Cyclic voltammograms of CNT fibers with diameters of 25, 40, 60, and 100 μm and a Pt wire with diameter of 25 μm using the T^-/T_2 electrolyte at a scan rate of 50 mV s^{-1}. The inset graph shows the peak-to-peak voltage separation (V_{pp}) for different CNT fiber diameters.

observed for the half-reaction $2T^- \rightleftarrows T_2 + 2e^-$. In the case of the Pt wire, however, the redox peaks could not be well-identified because of the poor catalytic activity. In contrast, the two redox peaks of the CNT fibers were clearly observed. In cyclic voltammetry, a higher reduction peak current (I_p) and lower peak-to-peak voltage separation (V_{pp}) indicate better catalytic activity for the electrodes.[28] Obviously, I_p rises with increasing diameter of the CNT fiber from 25 to 100 μm becausde of the increasing surface area. V_{pp} for the two redox peaks decreased with increasing diameter from 25 to 100 μm. In addition, no obvious decreases in current density or shifts in peak location were found for any of the CNT fibers after 10 cycles (Figures S7–S10).

To further understand the different catalytic activities of aligned CNT fibers with different diameters, electrochemical impedance spectroscopy (EIS) was used to study the dye-sensitized photovoltaic wire. As shown in Figure S11, two semicircles were generally observed in all of the plots. The left one corresponds to the interface charge-transfer resistance between the counter electrode and the electrolyte, while the right one represents the sum of the electrolyte resistance and the interface charge-transfer resistance between the working electrode and the electrolyte. The size of the first semicircle decreased with increasing diameter of the CNT fiber from 25 to 100 μm, indicating a decrease of the charge-transfer resistance. In other words, the CNT fibers with diameters of 60 and 100 μm result in lower resistances with higher catalytic activities. This conclusion agrees with the cyclic voltammetry results. As expected, the wire cell based on the 25 μm diameter Pt wire as the counter electrode showed a much higher resistance (Figure S12).

CNT materials were previously found to work efficiently as counter electrodes for the I^-/I_3^- redox couple. For instance, aligned CNT sheets or composite films produced even higher energy conversion efficiencies than the Pt counter electrode in planar DSCs.[29] Unexpectedly, these aligned CNT fibers exhibited even higher performances with the organic T^-/T_2 couple than the I^-/I_3^- couple. Dye-sensitized photovoltaic wires were compared using the same aligned CNT fiber with diameter of 60 μm as the counter electrode but different electrolytes (Figure 5 and Table 2). For the same composition of the two

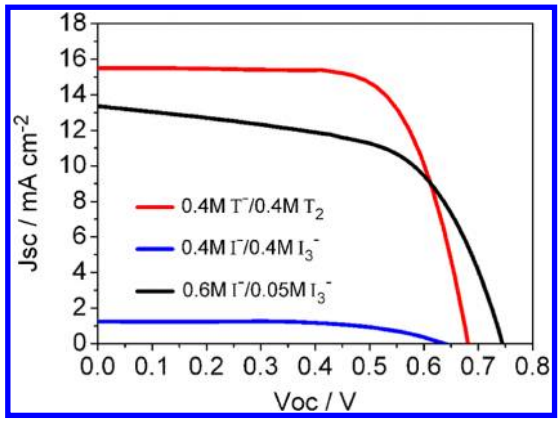

Figure 5. J–V curves of photovoltaic wires using T^-/T_2 or I^-/I_3^- as the redox couple with the same 60 μm diameter CNT fiber as the counter electrode, measured under AM 1.5 illumination.

Table 2. Photovoltaic Parameters in Figure 5

electrolyte	V_{oc} (mV)	J_{sc} (mA cm^{-2})	FF	η (%)
0.4 M T^-/0.4 M T_2	683	15.49	0.69	7.33
0.4 M I^-/0.4 M I_3^-	628	1.25	0.63	0.49
0.6 M I^-/0.05 M I_3^-	742	13.36	0.60	5.97

components (0.4 M for each) in the I^-/I_3^- and T^-/T_2 couples, the wire cell based on I^-/I_3^- showed much lower η of 0.49% compared with 7.33% for T^-/T_2. The lower η was mainly derived from the lower J_{sc}, which may be explained by the fact that the I^-/I_3^- electrolyte absorbs more visible light than the T^-/T_2 electrolyte (Figure S3). To decrease the absorbing effect, the composition of the I^-/I_3^- electrolyte was systematically optimized to finally increase the efficiency to 5.97%, which is still significantly lower than the value of 7.33% for the T^-/T_2 electrolyte. The above conclusion was further verified by EIS (Figures S13 and S14). The charge-transfer resistance at the counter electrode–electrolyte interface was much lower for the T^-/T_2 electrolyte than for the I^-/I_3^- electrolyte.

These photovoltaic wires exhibit high flexibility. They can be easily bent (Figure 6a,b) or even made into a knot (Figure S15) without breaking. Figure 6c compares the J–V curves for a photovoltaic wire made from a 60 μm diameter CNT fiber before and after bending, which overlap well. The high flexibility of the photovoltaic wire was further quantitatively studied by tracing the photovoltaic parameters (Figure 6d,e). The η values decreased slightly over the first 20 cycles and then were well-maintained in the following 80 cycles.

In summary, an organic thiolate/disulfide redox couple with low absorption in the visible region was developed for use in fabricating novel dye-sensitized photovoltaic wires. These flexible wire devices achieved high energy conversion efficiencies with a maximal value of 7.33%. This work also opens a new avenue in the development of highly efficient optoelectronic and electronic devices by designing matchable materials in different parts and making effective structures.

dx.doi.org/10.1021/ja405012w | J. Am. Chem. Soc. 2013, 135, 10622–10625

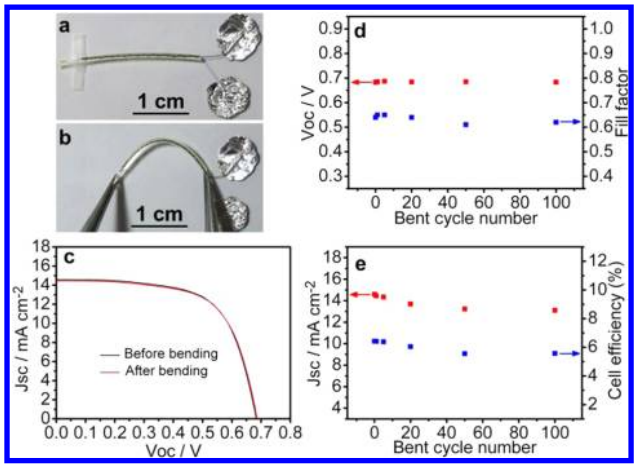

Figure 6. (a, b) Photographs of a photovoltaic wire (a) before and (b) after bending. (c) *J*–*V* curves of the photovoltaic wires before and after bending. (d, e) Photovoltaic parameters before and after different numbers of bending cycles.

■ ASSOCIATED CONTENT

Supporting Information

Synthesis of the organic electrolyte and structure and property characterizations of devices. This material is available free of charge via the Internet at http://pubs.acs.org.

■ AUTHOR INFORMATION

Corresponding Author

penghs@fudan.edu.cn

Notes

The authors declare no competing financial interest.

■ ACKNOWLEDGMENTS

This work was supported by NSFC (91027025, 21225417), MOST (2011CB932503, 2011DFA51330), STCSM (11520701400, 12nm0503200), the Fok Ying Tong Education Foundation, and The Program for Professor of Special Appointment at Shanghai Institutions of Higher Learning.

■ REFERENCES

(1) O'Regan, B.; Grätzel, M. *Nature* **1991**, *353*, 737.
(2) Zhu, K.; Neale, N. R.; Miedaner, A.; Frank, A. J. *Nano Lett.* **2007**, *7*, 69.
(3) Varghese, O. K.; Paulose, M.; Grimes, C. A. *Nat. Nanotechnol.* **2009**, *4*, 592.
(4) Hamann, T. W.; Ondersma, J. W. *Energy Environ. Sci.* **2011**, *4*, 370.
(5) Zhang, Q. F.; Dandeneau, C. S.; Zhou, X. Y.; Cao, G. Z. *Adv. Mater.* **2009**, *21*, 4087.
(6) Jennings, J. R.; Ghicov, A.; Peter, L. M.; Schmuki, P.; Walker, A. B. *J. Am. Chem. Soc.* **2008**, *130*, 13364.
(7) Martinson, A. B. F.; Hamann, T. W.; Pellin, M. J.; Hupp, J. T. *Chem.—Eur. J.* **2008**, *14*, 4458.
(8) Chen, T.; Qiu, L.; Yang, Z.; Peng, H. *Chem. Soc. Rev.* **2013**, *42*, 5031.
(9) Weintraub, B.; Wei, Y. G.; Wang, Z. L. *Angew. Chem., Int. Ed.* **2009**, *48*, 8981.
(10) Wang, M. K.; Chamberland, N.; Breau, L.; Moser, J. E.; Humphry-Baker, R.; Marsan, B.; Zakeeruddin, S. M.; Grätzel, M. *Nat. Chem.* **2010**, *2*, 385.
(11) Yella, A.; Lee, H. W.; Tsao, H. N.; Yi, C. Y.; Chandiran, A. K.; Nazeeruddin, M. K.; Diau, E. W. G.; Yeh, C. Y.; Zakeeruddin, S. M.; Grätzel, M. *Science* **2011**, *334*, 629.
(12) Daeneke, T.; Kwon, T. H.; Holmes, A. B.; Duffy, N. W.; Bach, U.; Spiccia, L. *Nat. Chem.* **2011**, *3*, 211.
(13) Yanagida, S.; Yu, Y. H.; Manseki, K. *Acc. Chem. Res.* **2009**, *42*, 1827.
(14) Li, D. M.; Li, H.; Luo, Y. H.; Li, K. X.; Meng, Q. B.; Armand, M.; Chen, L. Q. *Adv. Funct. Mater.* **2010**, *20*, 3358.
(15) Tian, H. N.; Jiang, X. A.; Yu, Z.; Kloo, L.; Hagfeldt, A.; Sun, L. C. *Angew. Chem., Int. Ed.* **2010**, *49*, 7328.
(16) Wu, M. X.; Lin, X.; Wang, Y. D.; Wang, L.; Guo, W.; Qu, D. D.; Peng, X. J.; Hagfeldt, A.; Grätzel, M.; Ma, T. L. *J. Am. Chem. Soc.* **2012**, *134*, 3419.
(17) Liu, G. H.; Li, X.; Wang, H.; Rong, Y. G.; Ku, Z. L.; Xu, M.; Liu, L. F.; Hu, M.; Yang, Y.; Han, H. W. *Carbon* **2013**, *53*, 11.
(18) Hao, F.; Wang, Z.; Luo, Q.; Lou, J.; Li, J. B.; Wang, J. P.; Fan, S. S.; Jiang, K. L.; Lin, H. *J. Mater. Chem.* **2012**, *22*, 22756.
(19) Hao, F.; Dong, P.; Zhang, J.; Zhang, Y. C.; Loya, P. E.; Hauge, R. H.; Li, J. B.; Lou, J.; Lin, H. *Sci. Rep.* **2012**, *2*, 368.
(20) Tian, H. N.; Yu, Z.; Hagfeldt, A.; Kloo, L.; Sun, L. *J. Am. Chem. Soc.* **2011**, *133*, 9413.
(21) Burschka, J.; Brault, V.; Ahmad, S.; Breau, L.; Nazeeruddin, M. K.; Marsan, B.; Zakeeruddin, S. M.; Grätzel, M. *Energy Environ. Sci.* **2012**, *5*, 6089.
(22) Chen, T.; Wang, S. T.; Yang, Z. B.; Feng, Q. Y.; Sun, X. M.; Li, L.; Wang, Z. S.; Peng, H. S. *Angew. Chem., Int. Ed.* **2011**, *50*, 1815.
(23) Baughman, R. H.; Zakhidov, A. A.; de Heer, W. A. *Science* **2002**, *297*, 787.
(24) Avouris, P.; Chen, Z. H.; Perebeinos, V. *Nat. Nanotechnol.* **2007**, *2*, 605.
(25) Avouris, P.; Freitag, M.; Perebeinos, V. *Nat. Photonics* **2008**, *2*, 341.
(26) Chen, T.; Qiu, L. B.; Kia, H. G.; Yang, Z. B.; Peng, H. S. *Adv. Mater.* **2012**, *24*, 4623.
(27) Zhang, S.; Ji, C. Y.; Bian, Z. Q.; Yu, P. R.; Zhang, L. H.; Liu, D. Y.; Shi, E. Z.; Shang, Y. Y.; Peng, H. T.; Cheng, Q.; Wang, D.; Huang, C. H.; Cao, A. Y. *ACS Nano* **2012**, *6*, 7191.
(28) Gong, F.; Wang, H.; Xu, X.; Zhou, G.; Wang, Z. S. *J. Am. Chem. Soc.* **2012**, *134*, 10953.
(29) Huang, S.; Yang, Z.; Zhang, L.; He, R.; Chen, T.; Cai, Z.; Luo, Y.; Lin, H.; Cao, H.; Zhu, X.; Peng, H. *J. Mater. Chem.* **2012**, *22*, 16833.